Astrophysics and Space Science (2023) 368:13
https://doi.org/10.1007/s10509-023-04169-3

RESEARCH

Continuation of some nearly circular symmetric periodic orbits in the elliptic restricted three-body problem

Xing-Bo Xu[1] · **Ye-Zhi Song**[2]

Received: 9 October 2022 / Accepted: 26 February 2023

Abstract
Some comet- and Hill-type families of nearly circular symmetric periodic orbits of the elliptic restricted three-body problem in the inertial frame are numerically explored by Broyden's method with a line search. Some basic knowledge is introduced for self-consistency. Set j/k as the period ratio between the inner and the outer orbits. The values of j/k are mainly $1/j$ with $2 \leq j \leq 10$ and $j = 15, 20, 98, 100, 102$. Many sets of the initial values of these periodic orbits are given when the orbital eccentricity e_p of the primaries equals 0.05. When the mass ratio $\mu = 0.5$, both spatial and planar doubly-symmetric periodic orbits are numerically investigated. The spacial orbits are almost perpendicular to the orbital plane of the primaries. Generally, these orbits are linearly stable when the j/k is small enough, and there exist linearly stable orbits when j/k is not small. If $\mu \neq 0.5$, there is only one symmetry for the high-inclination periodic orbits, and the accuracy of the periodic orbits is determined after one period. Some diagrams between the stability index and e_p or μ are supplied. For $\mu = 0.5$, we set $j/k = 1/2, 1/4, 1/6, 1/8$ and $e_p \in [0, 0.95]$. For $e_p = 0.05$ and 0.0489, we fix $j/k = 1/8$ and set $\mu \in [0, 0.5]$. Some Hill-type high-inclination periodic orbits are numerically studied. When the mass of the central primary is very small, the elliptic Hill lunar model is suggested, and some numerical examples are given.

Keywords Periodic orbits · Restricted three-body problem · Spatial resonance · Numerical continuation

1 Introduction

Periodic solutions play an important role in the study of the nonlinear dynamical phenomena in celestial mechanics. The closed trajectories in the phase space are also called periodic orbits. Infinitely many periodic orbits exist in the Kepler problem in the inertial frame or in the synodic frame, and they can be continued along a parameter according to Poincaré's continuation method under some assumptions. These periodic orbits usually form into one-parameter families, and the existence, stability, and bifurcations can be studied analytically and numerically (Szebehely 1967; Hénon 1997; Meyer et al. 2009).

In the restricted three-body problem (RTBP), two primaries move along their respective circular (CRTBP) or elliptic (ERTBP) orbits around their center of masses without any perturbations of the infinitesimal body, and the infinitesimal body as the research object is subjected to the gravitation of both primaries. The ERTBP model is very useful in space mission designs, as the orbits of the primaries are usually eccentric; for example, the eccentricity is about 0.205632 for Mercury, about 0.0934 for Mars, and about 0.0549 for the Moon. The ERTBP model is also a first-order model for describing the motion of an extrasolar planet around a binary system, see, e.g., Broucke (2001), Haghighipour et al. (2010).

Various kinds of periodic orbits of the RTBP in the rotating frame, including resonant orbits, quasi-collision orbits, and orbits around the librations, are being studied by many researchers. Unlike the conserved Hamiltonian system in which the energy can be served as a parameter, and one-parameter families exist according to the Cylinder theorem (Meyer et al. 2009; Galan-Vioque et al. 2014), the Hamiltonian of the ERTBP is periodic and not conserved. So, an external parameter is needed to obtain the one-parameter

✉ X.-B. Xu
xuxingbo25@hotmail.com

[1] Faculty of Mathematics and Physics, Huaiyin Institute of Technology, No. 1, Meicheng Road, Huai'An, 223003, Jiangsu, China

[2] Shanghai Astronomical Observatory, Chinese Academy of Sciences, No. 80, Nandan Road, Shanghai, 200030, Shanghai, China

Published online: 15 March 2023

families, and the parameter is usually the orbital eccentricity or the mass ratio of the primaries. In Sarris (1989), two groups of three-dimensional symmetric periodic orbits of the ERTBP are studied with the mass ratio and the eccentricity as the parameters. In Ollé and Pacha (1999), the periodic orbits of the planar isosceles RTBP, the Sitnikov and the MacMillan problems are numerically continued, and the stability of the families is studied. In Kotoulas and Voyatzis (2005), some exterior mean motion resonant periodic orbits with high inclinations are numerically studied using the Sun-Neptune ERTBP model. A review on the resonant periodic orbits can be found in Pan and Hou (2022). In Peng and Xu (2015), two groups of multi-revolution elliptic halo (ME-halo) orbits of the ERTBP are systematically calculated by the optimization method, and their linear stability is studied. In the Sun-Mercury ERTBP, Peng et al. (2017) also studied the ME-halo orbits around the Euler libration points near Mercury by the continuation of the resonant halo orbits. Sheth and Thomas (2022) applied the Lindstedt-Poincaré method to give the approximate solutions of the planar Lyapunov and three-dimensional halo orbits in the linear system of the ERTBP, computed the halo orbits in the Sun-Mars ERTBP by the differential correction method, and studied the effect of the solar radiation pressure on the bifurcations. The elliptic Hill problem model is more accurate than the circular Hill model for describing the motion of a satellite near a planet. A recent progress on the periodic orbits with stability regions in the elliptic Hill problem can be found in Voyatzis et al. (2012). For the study of the quasi-collision orbits of the RTBP, some references are Gómez and Ollé (1986), Llibre and Piñol (1990), Gomez and Olle (1991), Bolotin (2015), Zhao (2021).

Orbital elements are inevitably used to understand perturbed Keplerian orbits. The elliptic elements have the advantage of distinguishing the slow and fast variables. In Hamiltonian mechanics, canonical elements expressed by the orbital elements are usually used. Fast variables in the perturbation terms cause the short-period effects, which can be eliminated by the averaging method. As the ERTBP owns a time-reversing symmetry, some symmetric periodic orbits are proved to exist. Cors et al. (2001) showed the existence of a class of comet-type symmetric periodic orbits in the spatial ERTBP with the masses of the primaries equal. The restriction on the mass ratio of the primaries is removed by applying the averaging method and a generalized version of Arenstorf's theorem (Cors et al. 2005). These orbits are nearly circular, almost perpendicular to the reference plane, and can be described as of high inclination.

Note that the averaging method is used to simplify the perturbed terms with short-period effects. Palacián et al. (2006) gave six sets of the approximate initial values for searching the comet-type periodic orbits by calculating the equilibria of the averaged first-order system. Six equilibria correspond to six families of periodic orbits. Two families are planar, and the other four families are of high inclination. The existence of the Hill-type nearly circular periodic orbits with large inclinations is proved by Xu and Fu (2009). As there is a lack of numerical study on these comet- and Hill-type orbits with high inclinations, the aim of this paper is to calculate some orbits and study their linear stability numerically.

In the computing age, periodic orbits are continued near the known ones along a parameter or searched by the grid method. The theory of continuation is based on the implicit function theorem or the fixed point theorem, and the idea dates from the first work of H. Poincaré (1884) on the three-body problem (Chenciner 2015). The initial values of a periodic orbit can be numerically determined by the multiple shooting method (Farantos 1998). The periodicity conditions can be considered the nonlinear simultaneous equations, so Broyden's method can be applied (Broyden 1965). In Xu (2022), some continuation algorithms are reviewed, and a scheme is proposed for the continuation of both asymmetric and symmetric periodic solutions. The scheme combines the periodicity conditions and Broyden's method with a line search (Press et al. 1992). An application of this scheme can be found in Xu (2023) for the numerical study of the doubly symmetric periodic orbits of the CRTBP. If one wants to find more periodic orbits in a given set of initial values, the improved grid method using parallel computing can be applied (see, e.g., Tsirogiannis et al. 2009; Koh et al. 2021 and references therein).

Based on the preliminary work by Xu (2022, 2023), we consider the numerical continuation of some comet- and Hill-type three-dimensional nearly circular periodic orbits in the ERTBP and also study their linear stability. The paper is organized as follows. Section 2 introduces the Hamiltonian dynamical systems, the time-reversing symmetries, initial values of the approximate system, and how to calculate the linear stability of the periodic orbits. In Sect. 3, some numerical results are discussed. The last section summarizes the conclusions.

2 The models in the inertial frame

2.1 The Hamiltonian systems

In the spatial ERTBP, the infinitesimal body is subjected to the gravitational attraction of the primaries $\mathtt{P}_1$ and $\mathtt{P}_2$. Choose the unit system such that the semi-major axis of the relative elliptic orbit, the total mass of the primaries, and the gravitational constant are all equal to 1. In this unit system, $\mu \in (0, 1)$ and $1 - \mu$ are the masses of $\mathtt{P}_2$ and $\mathtt{P}_1$, respectively. It is easy to verify that the orbital period of the primary system is 2π. The center of masses is set as the origin of the inertial right-handed Cartesian coordinate frame

$O-u_1u_2u_3$, and the line of the semi-major axis is set as the u_1-axis. The motion plane of the primaries is set as the reference plane, and the axis u_3 is perpendicular to the reference plane. In this frame, the primaries rotate anticlockwise from the direction of the positive u_3-axis.

Let the upper T represent transposition. The position of the infinitesimal body is denoted as $\boldsymbol{q}=(q_1,q_2,q_3)^{\mathrm{T}}\in\mathbb{R}^3$. The vector from $\mathtt{P}_2$ to $\mathtt{P}_1$ is denoted as $\boldsymbol{d}=(d_1,d_2,0)^{\mathrm{T}}\in\mathbb{R}^3$. The position of $\mathtt{P}_2$ is $-(1-\mu)\boldsymbol{d}$, and the position of $\mathtt{P}_1$ is $\mu\boldsymbol{d}$. Suppose that there are no singularities, we have $R_1=\|\boldsymbol{q}-\mu\boldsymbol{d}\|>0$ and $R_2=\|\boldsymbol{q}+(1-\mu)\boldsymbol{d}\|>0$, where $\|\cdot\|$ is the Euclidean distance norm. The differential equation system is

$$\ddot{\boldsymbol{q}}=-\frac{(1-\mu)(\boldsymbol{q}-\mu\boldsymbol{d})}{R_1^3}-\frac{\mu(\boldsymbol{q}+(1-\mu)\boldsymbol{d})}{R_2^3}. \tag{1}$$

The vector $\boldsymbol{d}$ is a solution of the planar Kepler problem $\ddot{\boldsymbol{d}}=-\boldsymbol{d}\cdot\|\boldsymbol{d}\|^{-3}$. For the relative orbit of the primaries, let e_p denote the eccentricity, $E_p(t)$ denote the eccentric anomaly, $f_p(t)$ denote the true anomaly, and $M_p(t)=t$ denote the mean anomaly. $E_p(t)$ satisfies the Kepler equation $E_p-e_p\sin E_p=M_p(t)$, and $\boldsymbol{d}$ can be expressed as

$$\begin{aligned}\boldsymbol{d}&=d(\cos f_p,\sin f_p,0)^{\mathrm{T}}\\&=(\cos E_p-e_p,\sqrt{1-e_p^2}\sin E_p,0)^{\mathrm{T}},\end{aligned}$$

where $d=\|\boldsymbol{d}\|=1-e_p\cos E_p>0$. Denote the conjugate momentum as $\boldsymbol{p}=\dot{\boldsymbol{q}}$, and the Hamiltonian can be expressed as

$$\mathcal{H}^{\odot}=\frac{1}{2}\|\boldsymbol{p}\|^2-\frac{1-\mu}{R_1}-\frac{\mu}{R_2}. \tag{2}$$

For the comet-type orbits, the infinitesimal body is far away from both primaries. Denote $R=\|\boldsymbol{q}\|\gg 1$ and define $\cos\theta$ as

$$\cos\theta=R^{-1}\boldsymbol{q}\cdot\boldsymbol{d}/d=(q_1\cos f_p+q_2\sin f_p)/R. \tag{3}$$

The two potential function terms in (2) can be expanded into Legendre polynomial series:

$$\begin{aligned}&\frac{1-\mu}{R_1}+\frac{\mu}{R_2}\\&=\frac{1}{R}\sum_{l=0}^{\infty}\mathscr{P}_l(\cos\theta)\left[(1-\mu)\frac{(-\mu)^l}{R^l}+\mu\frac{(1-\mu)^l}{R^l}\right],\end{aligned}$$

where $\mathscr{P}_0(\cos\theta)=1$, $\mathscr{P}_1(\cos\theta)=\cos\theta$, $\mathscr{P}_2(\cos\theta)=\frac{3}{2}\cos^2\theta-\frac{1}{2}$ and

$$\mathscr{P}_l(-\cos\theta)=(-1)^l\mathscr{P}(\cos\theta),$$

$$\mathscr{P}_{l+1}(\cos\theta)=\frac{2l+1}{l+1}\cos\theta\mathscr{P}_l(\cos\theta)-\frac{l}{l+1}\mathscr{P}_{l-1}(\cos\theta),$$

$l\in\mathbb{N}$.

Neglecting the terms with $l\geq 1$, the approximate system of the full Hamiltonian system (2) for the comet-type orbits is

$$\mathcal{H}_0^{\odot}=\frac{1}{2}\|\boldsymbol{p}\|^2-\frac{1}{\|\boldsymbol{q}\|}. \tag{4}$$

To study the Hill-type motion near one primary, we move the origin to $\mathtt{P}_2$. Let $\boldsymbol{q}=\boldsymbol{x}-(1-\mu)\boldsymbol{d}$, then the system (1) becomes

$$\ddot{\boldsymbol{x}}-(1-\mu)\ddot{\boldsymbol{d}}=-\frac{\mu\boldsymbol{x}}{\|\boldsymbol{x}\|^3}-\frac{(1-\mu)(\boldsymbol{x}-\boldsymbol{d})}{\|\boldsymbol{x}-\boldsymbol{d}\|^3},$$

which is equivalent to

$$\ddot{\boldsymbol{x}}=\frac{\partial}{\partial\boldsymbol{x}}\left(\frac{\mu}{\|\boldsymbol{x}\|}+\frac{1-\mu}{\|\boldsymbol{x}-\boldsymbol{d}\|}-(1-\mu)\frac{\boldsymbol{d}\cdot\boldsymbol{x}}{d^3}\right). \tag{5}$$

The corresponding Hamiltonian can be expressed as

$$\mathcal{H}^{\mathtt{P}2}=\frac{1}{2}\|\boldsymbol{y}\|^2-\frac{\mu}{\|\boldsymbol{x}\|}-\frac{1-\mu}{\|\boldsymbol{x}-\boldsymbol{d}\|}+\frac{(1-\mu)\boldsymbol{x}\cdot\boldsymbol{d}}{d^3}, \tag{6}$$

with the conjugate momentum $\boldsymbol{y}=\dot{\boldsymbol{x}}$.

2.2 Canonical elements

The approximate system (4) and the system of the primaries constitute a double two-body problem. To understand the theoretically predicted periodic orbits of the full system, we introduce the orbital elements, which are semi-major axis a, eccentricity e, inclination i, longitude of the ascending node Ω, argument of the pericenter ω, and the mean-anomaly $M(t)=nt$. The mean motion n represents the average angular velocity of the orbit of the infinitesimal body. As i is not defined for planar orbits, and ω is not defined for circular orbits, some other forms of elements are used instead. The Poincaré-Delaunay elements ($Q_1=\ell+g$, $Q_2=\sqrt{L-G}\sin(-g)$, $Q_3=h$, $P_1=L$, $P_2=\sqrt{L-G}\cos(-g)$, $P_3=H$) are effective for the spatial circular orbits with high inclinations, where the Delaunay elements are $\ell(t)=M(t)$, $g=\omega$, $h=\Omega$, $L=\sqrt{a}$, $G=L\sqrt{1-e^2}$, $H=G\cos i$. Thus, the approximate system (4) can be expressed by the canonical elements as $\mathcal{H}_0^{\odot}=-\frac{1}{2a}=-\frac{1}{2L^2}$. These canonical elements are useful for theoretical analysis, although they do not seem as convenient as the Cartesian coordinates in our numerical work.

2.3 The perturbation

The difference between the full system (2) and the approximate system (4) is the perturbation for the comet-type motions. With the aim of estimating the order of the magnitude of the perturbation, a small parameter ε is introduced by the symplectic scaling method as $\boldsymbol{q}=\varepsilon^{-2}\tilde{\boldsymbol{q}}$, $\boldsymbol{p}=\varepsilon\tilde{\boldsymbol{p}}$. The size of ε^{-2} represents how far the infinitesimal body is away

from the center of masses. This is a symplectic transformation with multiplier ε. The scaled Hamiltonian $\tilde{\mathcal{H}}^{\odot} = \varepsilon \mathcal{H}^{\odot}$ can be written in series as

$$\tilde{\mathcal{H}}^{\odot} = \varepsilon^3 \left(\frac{1}{2} \|\tilde{\boldsymbol{p}}\|^2 - \frac{1}{\|\tilde{\boldsymbol{q}}\|} \right) - \varepsilon^7 \frac{\mu(1-\mu)}{\|\tilde{\boldsymbol{q}}\|^3} \mathscr{P}_2(\cos\theta) - \varepsilon^9 \frac{(1-2\mu)\mu(1-\mu)}{\|\tilde{\boldsymbol{q}}\|^4} \mathscr{P}_3(\cos\theta) - \mathcal{O}(\varepsilon^{11}). \tag{7}$$

So, the perturbation of the approximate system is of order ε^4 if $\mu(1-\mu)$ is not small, and the second term in the perturbation is zero if $\mu = 0.5$.

To estimate the perturbation of the orbit near the primary $\mathtt{P}_2$, let the size of ε represent how close to $\mathtt{P}_2$ the infinitesimal body is. Let $\boldsymbol{x} = \varepsilon^2 \mu^{1/3} \tilde{\boldsymbol{x}}$, $\boldsymbol{y} = \varepsilon^{-1} \mu^{1/3} \tilde{\boldsymbol{y}}$, which is a symplectic change of variables with multiplier $\varepsilon^{-1}\mu^{-2/3}$. The scaled Hamiltonian $\tilde{\mathcal{H}}^{\mathtt{P}2}$ can be written as

$$\begin{aligned}\tilde{\mathcal{H}}^{\mathtt{P}2} &= \varepsilon^{-3} \left(\frac{1}{2} \|\tilde{\boldsymbol{y}}\|^2 - \frac{1}{\|\tilde{\boldsymbol{x}}\|} \right) - \varepsilon^{-1} \frac{\mu^{-2/3}(1-\mu)}{\|\varepsilon^2 \mu^{1/3} \tilde{\boldsymbol{x}} - \boldsymbol{d}\|} \\ &\quad + \varepsilon \mu^{-1/3} \frac{(1-\mu)\tilde{\boldsymbol{x}} \cdot \boldsymbol{d}}{d^3} \\ &= \varepsilon^{-3} \left(\frac{1}{2} \|\tilde{\boldsymbol{y}}\|^2 - \frac{1}{\|\tilde{\boldsymbol{x}}\|} \right) - \varepsilon^3 (1-\mu) \frac{\|\tilde{\boldsymbol{x}}\|^2}{d^3} \mathscr{P}_2(\cos\theta) \\ &\quad + \mathcal{O}(\mu^{1/3} \varepsilon^5). \end{aligned} \tag{8}$$

So, the perturbation order of the approximate system in the Hamiltonian system $\tilde{\mathcal{H}}^{\mathtt{P}2}$ is of order ε^6.

2.4 Symmetries

There exist symmetries in the ERTBP. The symmetry may be about the u_1-axis, the u_1u_3-plane, or the u_1u_2-plane (Broucke 2001). Symmetries are exploited to provide the periodicity conditions of the symmetric periodic orbits. The first symmetry about the u_1-axis corresponds to the time-reversing symmetry $\mathscr{R}_1$, which is usually applied in the spatial ERTBP. The second symmetry about the u_1u_3-plane is mostly used for the planar periodic orbits in the ERTBP, and the time-reversing symmetry is denoted as $\mathscr{R}_2$. The third symmetry about the u_1u_2-plane is usually used in the vertical motion problems and is out of our scope here.

$$\begin{aligned}&\mathscr{R}_1 : (q_1, q_2, q_3, p_1, p_2, p_3, E_p(t), t) \\ &\quad \to (q_1, -q_2, -q_3, -p_1, p_2, p_3, -E_p(t), -t), \\ &\mathscr{R}_2 : (q_1, q_2, q_3, p_1, p_2, p_3, E_p(t), t) \\ &\quad \to (q_1, -q_2, q_3, -p_1, p_2, -p_3, -E_p(t), -t).\end{aligned}$$

The periodicity conditions for the nearly circular $\mathscr{R}_1$-symmetric periodic orbits are based on the following well-known proposition (Cors et al. 2005).

Proposition 1 *Consider the general ERTBP as described by the Hamiltonian system (2) or (6) as above. Let* $\mathscr{L}_1 = \{(\boldsymbol{q}, \boldsymbol{p}, t) : q_2 = q_3 = p_1 = 0, t = 0 \mod \pi\}$ *if a solution starts from* $\mathscr{L}_1$ *and comes back to* $\mathscr{L}_1$ *after a time* $T/2 = k\pi > 0$. *Then* (1) *the solution is a periodic orbit with period* $T = 2k\pi$; (2) *the Lagrangian set* $\mathscr{L}_1$ *is equivalent to* $\mathscr{L}_1^{(1)}$, *in which* $\sin i > 0$ *and*

$$\mathscr{L}_1^{(1)} = \{(Q, P, t) : Q_1 = 0 \mod \pi, \quad Q_2 \equiv 0, \quad Q_3 = 0 \mod \pi, \quad t = 0 \mod \pi\}.$$

Proof (1) Denote the solution of the Hamiltonian system (2) or (6) as $Z(t, Z_0) = (\boldsymbol{q}, \boldsymbol{p})$ with $Z_0 \in \mathscr{L}_1$. Define the anti-symplectic matrix $\Gamma_1 = \mathbf{diag}\{1, -1, -1, -1, 1, 1\}$, then we have $\Gamma_1 Z_0 = Z_0$. According to the $\mathscr{R}_1$-symmetry, we have

$$\Gamma_1 Z(-t, Z_0) = Z(t, Z_0). \tag{9}$$

Set $t = k\pi$. As $Z(k\pi, Z_0) \in \mathscr{L}_1$, then $\Gamma_1 Z(k\pi, Z_0) = Z(k\pi, Z_0)$. Combining with the equation (9), we have $\Gamma_1^2 Z(-k\pi, Z_0) = Z(-k\pi, Z_0) = Z(k\pi, Z_0)$. Thus, the solution is periodic with period $2k\pi$.

(2) As $q_3 = r \sin(f+\omega) \sin i$ and $\sin i > 0$, we have $f + \omega = 0 \mod \pi$ in the set $\mathscr{L}_1$. As $q_2 = \cos(f+\omega)\sin\Omega + \cos i \sin(f+\omega)\cos\Omega$, then $\Omega = 0 \mod \pi$ in the set $\mathscr{L}_1$. As

$$\begin{aligned}\dot{q}_1 = &-\frac{C_k}{a(1-e^2)} \\ &\times \big[(\sin(f+\omega)\cos\Omega + \cos i \sin\Omega \cos(f+\omega)) \\ &+ e(\sin\omega\cos\Omega + \cos i \cos\omega \sin\Omega)\big],\end{aligned}$$

then $e \sin\omega = 0$ in the set $\mathscr{L}_1$. According to the definition of the Poincaré-Delaunay elements, $\mathscr{L}_1$ is equivalent to $\mathscr{L}_1^{(1)}$. □

In the ERTBP with $\mu = 1/2$, there exist solutions symmetric with respect to the u_2u_3-plane (the fourth) or the u_2-axis (the fifth). Corresponding to the fourth symmetry, the time-reversing symmetry $\mathscr{R}_4$ is

$$\begin{aligned}&\mathscr{R}_4 : (q_1, q_2, q_3, p_1, p_2, p_3, E_p(t), t) \\ &\quad \to (-q_1, q_2, q_3, p_1, -p_2, -p_3, -E_p(t), -t).\end{aligned}$$

The Lagrangian set $\mathscr{L}_4$ is defined as below

$$\mathscr{L}_4 = \{(\boldsymbol{q}, \boldsymbol{p}, t) : q_1 = p_2 = p_3 = 0, t = 0 \mod \pi\}.$$

It is easy to verify that this set is equivalent to

$$\mathscr{L}_4^{(1)} = \{(Q, P, t) : Q_1 = \frac{\pi}{2} \mod \pi, \quad Q_3 = 0 \mod \pi, P_2 \equiv 0, t = 0 \mod \pi\}.$$

As is shown in Cors et al. (2001), there exists a class of $\mathscr{R}_1\mathscr{R}_4$-symmetric periodic orbits.

Proposition 2 *Let $Z(t, Z_0) = (\boldsymbol{q}, \boldsymbol{p})$ be a solution of the Hamiltonian system (2) with $\mu = 1/2$. If a solution $Z(t, Z_0)$ starts from $\mathscr{L}_1$ (or $\mathscr{L}_4$) at $t = 0$ and goes through $\mathscr{L}_4$ (or $\mathscr{L}_1$) at time $t = k_1\pi$ with $k_1 \in \mathbb{N}$ large, then the solution $Z(t, Z_0)$ is periodic with the period $4k_1\pi$.*

Proof The anti-symplectic matrix Γ_1 is defined in Proposition 1. Define the other anti-symplectic matrix $\Gamma_4 = \mathbf{diag}(-1, 1, 1, 1, -1, -1)$

$$\Gamma_1\Gamma_4 = -\mathbf{I}_6 = -\mathbf{diag}(1, 1, 1, 1, 1, 1), \quad \Gamma_1^2 = \Gamma_4^2 = \mathbf{I}_6.$$

Suppose $Z_0 \in \mathscr{L}$ at $t = 0$ and $Z_1 = Z(k\pi, Z_0) \in \mathscr{L}_3$ at $t = k_1\pi$. We have

$$\Gamma_1 Z_0 = Z_0, \quad \Gamma_4 Z_1 = Z_1, \quad \Gamma_1 Z_1 = \Gamma_4 Z(-k_1\pi, Z_0).$$

Then

$$\Gamma_1^2 Z_1 = \Gamma_1\Gamma_4 Z(-k_1\pi, Z_0) \iff Z_1 = -Z(-k_1\pi, Z_0).$$

Similarly, we have

$$Z(3k_1\pi, Z_0) = Z(2k_1\pi, Z_1) = -Z_1 = Z(-k_1\pi, Z_0),$$

and the period is $4k_1\pi$. □

2.5 Initial values

For the comet-type orbits, the approximate system (4) behaves like the outer orbit system, while the system of the two primaries is like the inner orbit system. The mean anomaly of the outer orbit changes much slower than that of the inner orbit. Let j and k be relatively prime integers. Suppose the infinitesimal body revolves around the origin j circles, and the primaries revolves around each other k circles. The period of a periodic solution is $2k\pi$ unit time. So, we have $|n|2k\pi = 2j\pi$ and $|n| = j/k$.

Note that $j \ll k$ is for the comet-type motions, and $j \gg k$ for the Hill-type motions. The initial values for the nearly circular $\mathscr{R}_1$-symmetric periodic orbits, which are almost perpendicular to the orbital plane of the primaries, can be written as

$$\begin{aligned}&(q_1, q_2, q_3, p_1, p_2, p_3, E_p(0))\\ &\quad = (\pm a + \delta_1, 0, 0, 0, \delta_2, na + \delta_3, E_p(0)),\end{aligned} \tag{10}$$

where $E_p(0) = 0$ or π, $a = (k/j)^{2/3}$ and δ_j is in a neighborhood of zero for $j = 1, 2, 3$. Theoretically, ε should be small, however, for the convenience of computing, we would like ε^3 not to be too small. To make scaled semi-major axis be 1, we set $\varepsilon^3 = j/k$ for the comet-type orbits with $n^2a^3 = 1$ and set $\varepsilon^3 = k/j$ for the Hill-type orbits with $n^2a^3 = \mu$. Then the initial values for both the comet- and Hill-type orbits have the same form as (10).

$\mathscr{R}_1\mathscr{R}_4$-symmetry exists in the ERTBP when $\mu = 0.5$. For the reason of this double symmetry, k should be even, and only $k_1\pi = k\pi/2$ unit time is needed to determine the doubly symmetric periodic orbits. If the initial values belong to the set $\mathscr{L}_1$, then the periodicity conditions are

$$\begin{aligned}&q_1(k_1\pi, q_1, p_2, p_3) = 0, \quad p_2(k_1\pi, q_1, p_2, p_3) = 0,\\ &p_3(k_1\pi, q_1, p_2, p_3) = 0.\end{aligned} \tag{11}$$

If the initial values belong to the set $\mathscr{L}_4$ as

$$\begin{aligned}&(q_1, q_2, q_3, p_1, p_2, p_3, E_p(0))\\ &\quad = (0, \delta_2, \pm a + \delta_1, na + \delta_3, E_p(0)),\end{aligned} \tag{12}$$

then the periodicity conditions are

$$\begin{aligned}&q_2(k_1\pi, q_2, q_3, p_1) = 0, \quad q_3(k_1\pi, q_2, q_3, p_1) = 0,\\ &p_1(k_1\pi, q_2, q_3, p_1) = 0.\end{aligned} \tag{13}$$

Consider the $\mathscr{R}_1$-symmetric Kepler circular-orbit solutions in the approximate system (4) as the approximate solutions of the periodicity conditions (11) or (13). The initial values satisfy $p_2(0) = 0$ if the solution starts from $\mathscr{L}_1$. The set of initial values in $\mathscr{L}_1$ can be represented as $(q_1, p_3, \cos E_p(0))$ with $E_p(0) = 0 \bmod \pi$, and there are generally eight cases for the signs listed as $(\pm, \pm, \pm)$. If the initial values belong to the set $\mathscr{L}_4$, the solutions satisfy $q_2(0) = 0$, and the set of initial values can be represented as $(q_3, p_1, \cos E_p(0))$. When $\mu = 0.5$, the number of the cases of the initial values is halved as the result of the symmetries, and only $q_1 > 0$ is considered.

2.6 Linear stability

Let $U = U(\boldsymbol{q}, t)$ be the time-dependent potential function $U = \frac{1-\mu}{R_1} + \frac{\mu}{R_2}$, then the differential system (1) can be rewritten as $\dot{\boldsymbol{q}} = \boldsymbol{p}$ and $\dot{\boldsymbol{p}} = \frac{\partial U}{\partial \boldsymbol{q}} = \nabla U$. The linearized differential equations of the system (1) can be written as

$$\delta\dot{\boldsymbol{q}} = \delta\boldsymbol{p}, \quad \delta\dot{\boldsymbol{p}} = \frac{\partial}{\partial \boldsymbol{q}^{\mathrm{T}}}\left(\frac{\partial U}{\partial \boldsymbol{q}}\right)\cdot\delta\boldsymbol{q} = \left(\nabla^2 U\right)\delta\boldsymbol{q}, \tag{14}$$

where $\delta\boldsymbol{q}, \delta\boldsymbol{p} \in \mathbb{R}^3$ and $\nabla^2 U$ is denoted as the Hessian matrix of U at $\boldsymbol{q}$. Set $\delta\boldsymbol{x}, \delta\boldsymbol{y} \in \mathbb{R}^3$, and the linearized differential system of the system (5) is

$$\begin{aligned}&\delta\dot{\boldsymbol{x}} = \delta\boldsymbol{y},\\ &\delta\dot{\boldsymbol{y}} = \mu\nabla^2\left(\frac{1}{\|\boldsymbol{x}\|}\right)\delta\boldsymbol{x} + (1-\mu)\nabla^2\left(\frac{1}{\|\boldsymbol{x}-\boldsymbol{d}\|}\right)\delta\boldsymbol{x}.\end{aligned} \tag{15}$$

The linearized procedure can be proceeded by referring to the calculation of the symmetric Hessian matrix below

$$\nabla^2\left(\frac{1}{\|\boldsymbol{x}-\boldsymbol{d}\|}\right) = -\nabla\left(\frac{\boldsymbol{x}-\boldsymbol{d}}{\|\boldsymbol{x}-\boldsymbol{d}\|^3}\right) =$$

$$\begin{pmatrix} \frac{3(x_1-d_1)^2-\|\boldsymbol{x}-\boldsymbol{d}\|^2}{\|\boldsymbol{x}-\boldsymbol{d}\|^5} & \frac{3(x_1-d_1)(x_2-d_2)}{\|\boldsymbol{x}-\boldsymbol{d}\|^5} & \frac{3(x_1-d_1)x_3}{\|\boldsymbol{x}-\boldsymbol{d}\|^5} \\ \frac{3(x_2-d_2)(x_1-d_1)}{\|\boldsymbol{x}-\boldsymbol{d}\|^5} & \frac{3(x_2-d_2)^2-\|\boldsymbol{x}-\boldsymbol{d}\|^2}{\|\boldsymbol{x}-\boldsymbol{d}\|^5} & \frac{3(x_2-d_2)x_3}{\|\boldsymbol{x}-\boldsymbol{d}\|^5} \\ \frac{3(x_1-d_1)x_3}{\|\boldsymbol{x}-\boldsymbol{d}\|^5} & \frac{3(x_2-d_2)x_3}{\|\boldsymbol{x}-\boldsymbol{d}\|^5} & \frac{3x_3^2-\|\boldsymbol{x}-\boldsymbol{d}\|^2}{\|\boldsymbol{x}-\boldsymbol{d}\|^5} \end{pmatrix}.$$

The linear stability can be determined by the characteristic multipliers calculated from the integration of these linearized differential equations with the identity matrix $\mathbf{I}_6$ as the initial matrix solution. The linear stability of a doubly symmetric periodic orbit can be known from the information of only one-fourth period. The proposition about the monodromy matrices of the symmetric periodic orbits can be expressed as below.

Proposition 3 (See Xu 2023 for the proof) *Let* $\mathcal{Z}(t, Z_0) \in \mathbb{R}^{6\times 6}$ *be the standard fundamental matrix solution of the system* (14). (1) *If* $Z(t, Z_0)$ *starts from* $\mathscr{L}_1$ *and comes back to* $\mathscr{L}_1$ *after time* $k\pi$ $(k \in \mathbb{N})$, *then the monodromy matrix can be calculated as*

$$\mathcal{Z}(2k\pi, Z_0) = \mathcal{Z}(k\pi, Z_0)\Gamma_1\mathcal{Z}^{-1}(k\pi, Z_0)\Gamma_1.$$

(2) $\mathscr{R}_1\mathscr{R}_4$*-symmetric periodic solutions exist when* $\mu = 0.5$ *in the system* (1). *The monodromy matrix for such a doubly symmetric* $4k_1\pi$*-period periodic solution with* $Z_0 \in \mathscr{L}_1$ *can be written as*

$$\mathcal{Z}(4k_1\pi, Z_0) = [\mathcal{N}(2k_1\pi, Z_0)\Gamma_1]^2,$$

where $k_1 \in \mathbb{N}$ *and*

$$\mathcal{N}(2k_1\pi, Z_0) = \mathcal{Z}(k_1\pi, Z_0)\Gamma_4\mathcal{Z}^{-1}(k_1\pi, Z_0).$$

If $Z_1 \in \mathscr{L}_4$, *the monodromy matrix* $\mathcal{Z}(4k_1\pi, Z_1)$ *satisfies*

$$\mathcal{Z}(4k_1\pi, Z_1) = [\mathcal{N}(2k_1\pi, Z_1)\Gamma_4]^2,$$

$$\mathcal{N}(2k_1\pi, Z_1) = \mathcal{Z}(k_1\pi, Z_1)\Gamma_1\mathcal{Z}^{-1}(k_1\pi, Z_1).$$

The eigenvalues of the monodromy matrix are called the (characteristic) multipliers and are in reciprocal pairs. If all the multipliers are not ± 1 and are on the unit circle with all the moduli equal to 1, then the corresponding periodic orbit is said to be linearly stable. A numerical experiment shows that some real multipliers can appear outside the unit circle, and no phenomena about the complex instability appear. The linear stability indicator ρ of a periodic orbit is denoted as the sum of the moduli of the six characteristic multipliers. There will be errors in the numerical calculations, so we take 10 significant digits for ρ to estimate the linear stability.

3 Numerical continuation

In this section, some numerical results about the comet- and Hill-type nearly circular symmetric periodic orbits are provided. The initial values of the periodic orbits are continued from those of the Kepler circular orbits, and the continued orbits are very close to the unperturbed orbits.

The integrations of the Cartesian coordinate differential equations (1) and (5) are executed by the variable step-size Runge-Kutta 7-8 routine. To continue the Kepler periodic orbits, we need to solve the periodicity conditions, which are achieved by the numerical integration from the initial values over the fixed time. Newton's method has its shortcomings in solving the simultaneous nonlinear equations, but Broyden's method with a line search converges globally and can overcome the shortcomings to a great degree (Broyden 1965). Although the corresponding routines in Press et al. (1992) can try many times to avoid the degeneracy of the Jacobian matrix, there are still some factors affecting the results, for example, the complicated perturbations, the inaccurate initial values, the errors brought by the integration, the inappropriate setting of the control parameters, and so on. The accuracy of the continued initial values is represented as the infinity norm of the deviation vector in the periodicity conditions of one period.

3.1 Comet-type

3.1.1 Equal-mass case

The Hamiltonian (2) with $\mu = 0.5$ has five types of time-reversing symmetry, which are about the u_1-axis ($\mathscr{R}_1$), the u_1u_3-plane ($\mathscr{R}_2$), the u_1u_2-plane, the u_2u_3-plane ($\mathscr{R}_4$), and the u_2-axis. Note that the first three types are valid for all the mass ratios, and the last two types are only valid for $\mu = 0.5$. Consider the numerical continuation of the $\mathscr{R}_1\mathscr{R}_4$-symmetric periodic orbits stated in Proposition 2. The cases of the approximate initial values is 8 if $\mu = 0.5$ and j/k is fixed, and there are 16 cases for the initial values of the continued orbits. According to the symmetries, the families of the continued orbits are symmetric with respect to the u_1u_2-plane. In Table 1, the initial values of some doubly symmetric periodic orbits, which are almost perpendicular to the reference plane, are calculated. Ten values of j/k are $1/2, 1/4, 1/6, 1/8, 1/10, 1/98, 1/100, 1/102$, and $3/8, 3/10$. The eccentricity e_p is chosen to be 0.05. The results are in good precision up to 10^{-12}. The numerical results show that the continued periodic orbits are almost accordingly symmetric if the approximate initial solutions are symmetric. The doubly symmetric periodic orbits can start from either the set $\mathscr{L}_1$ or the set $\mathscr{L}_4$, and the initial values to be continued can be referred to (10)–(13) in Sect. 2.5.

The accurate initial values of the case "$(1/102, +, +, -)$" can not be successfully found at first but later can be refined according to the initial values of the case "$(1/102, +, -, -)$" because of the symmetry $\mathscr{R}_1$. This special example reveals the fact that retrograde orbits are generally more stable than the prograde orbits. The stability index ρ also supports this

Table 1 Continuation results for the doubly symmetric comet-type periodic orbits with $\mu = 0.5, e_p = 0.05$. Ten mean motions $|n|\, j/k$ are considered. The signs "±, ±, ±" represent the signs of initial parameters q_1, $p_3, \cos E_p$. The accuracy is denoted as the infinity norm of the deviation vector of the periodic orbit after integrating a period

$j/k, q_1, p_3, \cos E_p$	q_1	p_2	p_3	ρ
1/2, +, ±, +	1.6408106616065017	3.9486472368497637E-2	±0.75000894569632204	12.29160706
1/2, +, ±, −	1.6548532537981551	-8.2730199360359608E-2	±0.76439150276818235	13.14353377
1/4, +, ±, +	2.5149127499795325	-1.1098202336745199E-3	±0.63433012391436261	6.031736506
1/4, +, ±, −	2.5331260778528937	-7.0753287981097836E-3	±0.62851132825771361	6.149820948
1/6, +, ±, +	3.3017164963159429	-1.0592239113123513E-3	±0.55206105150165152	6.000143326
1/6, +, ±, −	3.3048689435187657	-2.0209508948591088E-3	±0.55120133109681824	6.002095678
1/8, +, ±, +	4.0001649312745222	-5.183263762487362E-4	±0.50102581944331770	6.000067086
1/8, +, ±, −	4.0012170189086582	-9.327207960167349E-4	±0.50078986896828870	6.000082987
3/8, +, ±, +	2.0387333481595920	-1.2249115391472193E-2	±0.68773512110028778	6.236348792
3/8, +, ±, −	1.8612261365955991	-3.2155891051545454E-2	±0.74178298548701183	6.022658713
1/10, +, ±, +	4.6417627911543295	-2.898111919165371E-4	±0.46486060044136912	6.000037085
1/10, +, ±, −	4.6422788219070110	-5.138383815727713E-4	±0.46476525731277796	6.000037167
3/10, +, ±, +	2.1932339232083935	-2.2449496528567660E-3	±0.68481992354348842	6.013018795
3/10, +, ±, −	2.2832352999532248	-6.1797092118348234E-3	±0.65503917680311075	6.004385296
1/98, +, ±, +	21.256159310917599	-6.6947238777544310E-7	±0.21691474756871523	6.000000085
1/98, +, ±, −	21.256160292067928	-1.1592311093406933E-6	±0.21691472837150805	6.000000085
1/100, +, ±, +	21.544382923711527	-6.3435652947157414E-7	±0.21545848971781834	6.000000080
1/100, +, ±, −	21.544383853326160	-1.0984137028383664E-6	±0.21545847189277662	6.000000080
1/102, +, ±, +	21.830691300630864	-6.0172437560896545E-7	±0.21404056960035289	6.000000076
1/102, +, +, −	21.830691300630587	-6.0172530592989976E-7	0.21404056960035311	6.000000076
1/102, +, −, −	21.830692182360249	-1.0418987513387589E-6	-0.21404055302503697	6.000000076
$j/k, q_3, p_1, \cos E_p$	q_2	q_3	p_1	ρ
1/2, +, ±, +	±8.1415598484332066E-2	1.5116210866748250	±0.79542643068716523	13.14353689
1/2, +, ±, −	∓0.15262102153333548	1.4885849649577847	±0.79122085488058336	12.29160706
1/4, +, ±, +	∓9.3972457029645982E-3	2.5015227304858634	±0.61855295536688726	6.031736506
1/4, +, ±, −	±1.0439751255182444E-3	2.4873139000781608	±0.62390005099140422	6.149820948
1/6, +, ±, +	∓4.4426232102857054E-4	3.2835176686439334	±0.54548241845816170	6.002095678
1/6, +, ±, −	∓9.5214847590999554E-4	3.2823296161893540	±0.54592993580692606	6.000143326
1/8, +, ±, +	∓1.7181491030619797E-4	3.9846097404640073	±0.49703305450132229	6.000067086
1/8, +, ±, −	∓2.8017113105325853E-4	3.9841317652022674	±0.49718225480716838	6.000082987
3/8, +, ±, +	±1.9738916833429394E-2	1.7894281106224443	±0.73693807093704988	6.236348792
3/8, +, ±, −	±5.7921564123867304E-3	1.9935950656593973	±0.67522154849390625	6.022658713
1/10, +, ±, +	∓7.2759986171943558E-5	4.6282480606300416	±0.46212312398756367	6.000037167
1/10, +, ±, −	∓1.2090274887253335E-4	4.6280240829437922	±0.46218486827595667	6.000037085
3/10, +, ±, +	∓1.2219471542000060E-2	2.2419347344503953	±0.64391399536050842	6.004385296
3/10, +, −, −	1.7391573195070807E-2	2.1635836091208533	−0.67146379901960906	6.013018794
1/98, +, ±, +	∓1.5956665888980855E-8	21.253189872594007	±0.21685412863617834	6.000000085
1/98, +, ±, −	∓2.7019426742086156E-8	21.253189504148970	±0.21685414154064059	6.000000085
1/100, +, ±, +	∓1.4801154750361152E-8	21.541453203408832	±0.21539987822500106	6.000000080
1/100, +, ±, −	∓2.5091008768336938E-8	21.541452854334821	±0.21539989020792091	6.000000080
1/102, +, ±, +	∓1.3763602893106173E-8	21.827799996373994	±0.21398386125536917	6.000000076
1/102, +, ±, −	∓2.3332753592532629E-8	21.827799665297761	±0.21398387239887426	6.000000076

fact if ρ is expressed by 16 significant digits. The results show that such periodic orbits tend to be linearly stable as j/k decreases. The closer to 6 is the stability index ρ, the more stable the periodic orbit. To understand the graphics of such periodic orbits, two groups of graphics are shown in Fig. 1 and Fig. 2.

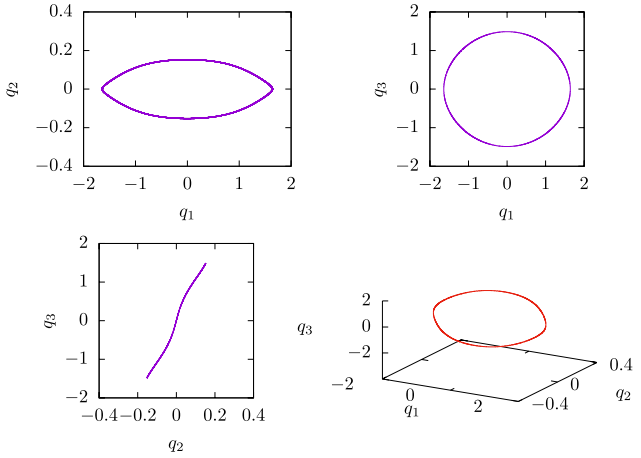

Fig. 1 The comet-type doubly symmetric periodic orbit with $\mu = 0.5$ and $e_p = 0.05$ for the case "$(1/2, +, +, +)$" in Table 1

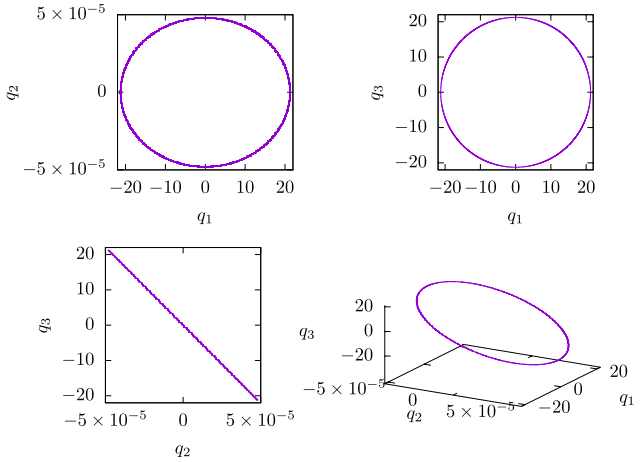

Fig. 2 The comet-type doubly symmetric periodic orbit with $\mu = 0.5$ and $e_p = 0.05$ for the case "$(1/98, +, +, -)$" in Table 1

If j/k and e_p are changed, the above procedure can be repeated. For the fixed case "$(j/k, +, -, +)$", the one-parameter families of periodic orbits can be continued along the parameter e_p from the same approximate initial solution. To show the relation between e_p and ρ, we offer some graphics for $j/k = 1/2, 1/4, 1/6, 1/8$ in Fig. 3. We set $0 \le e_p \le 0.95$ with the step 0.05 and find that ρ grows as e_p increases when e_p is small. When $j/k \le 1/8$, there is an inflection point at which ρ gets the maximum.

We find that some planar symmetric periodic orbits of the family l (comet-type direct motion) and m (comet-type retrograde motion) exist in the ERTBP, and the families can be continued along the eccentricity e_p. The notations $\mathrm{I}_{\mathrm{d}}^{\mathrm{j/k}}(e_p)$ and $\mathrm{I}_{\mathrm{r}}^{\mathrm{j/k}}(e_p)$ separately represent the families l and m. We calculate some planar $\mathscr{R}_1\mathscr{R}_2$-symmetric periodic orbits. The graphics of some orbits with $j = 1$, $2 \le k \le 5$ and $E_p = 0$ are shown in Fig. 4. The approximate initial values satisfy $(q_1, 0, 0, 0, p_2, 0)$ with $q_1 > 0$. From inside to outside of

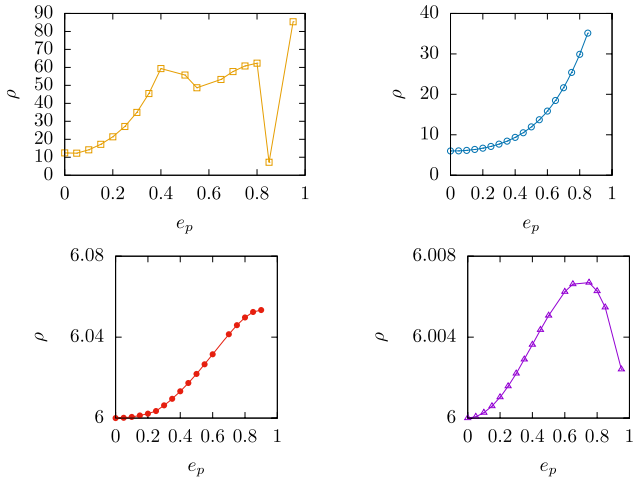

Fig. 3 The diagrams for the relations between the eccentricity e_p and the linear stability index ρ with e_p as the parameter. In the four subimages, $j/k = 1/2, 1/4, 1/6, 1/8$, respectively. Each family is of the case "$+, -, +$"

the left subgraph, the orbits are of type $\mathrm{I}_{\mathrm{r}}^{1/2}(0.5)$, $\mathrm{I}_{\mathrm{d}}^{1/3}(0.5)$, $\mathrm{I}_{\mathrm{r}}^{1/4}(0.5)$, $\mathrm{I}_{\mathrm{d}}^{1/5}(0.5)$, and $\mathrm{I}_{\mathrm{r}}^{1/5}(0.5)$. In the right subgraph, the $e_p - \rho$ relations of some cases are shown. "kr" represents the type $\mathrm{I}_{\mathrm{r}}^{1/k}$, and "$k$d" represents the type $\mathrm{I}_{\mathrm{d}}^{1/k}$. Generally speaking, orbits of family m are more stable than orbits of family l for the same semi-major axes. Periodic orbits of ${\mathrm{I}_{\mathrm{d}}}^{1/3}$ and ${\mathrm{I}_{\mathrm{d}}}^{1/4}$ are linearly stable when $e_p = 0$, but they become unstable quickly when $e_p > 0$. Family $\mathrm{I}_{\mathrm{r}}^{1/3}$ is weak linearly stable when $0.05 \le e_p \le 0.2$ as $\rho(0.15) \approx 6.0000015$ and unstable when $e_p > 0.55$. The continued orbit for the case $\mathrm{I}_{\mathrm{d}}^{1/2}(0)$ is very unstable as $\rho \approx 5465.0$. Family $\mathrm{I}_{\mathrm{r}}^{1/2}$ is linearly stable for $e_p \le 0.8$. Family $\mathrm{I}_{\mathrm{d}}^{1/6}$ becomes unstable when $e_p = 0.4$, and the maximum value of ρ is 6.19 when $e_p = 0.9$. Family $\mathrm{I}_{\mathrm{r}}^{1/6}$ is always linearly stable. The $e_p - \rho$ curves of the families ${\mathrm{I}_{\mathrm{d}}}^{1/5}$ and ${\mathrm{I}_{\mathrm{r}}}^{1/5}$ are not drawn. Family ${\mathrm{I}_{\mathrm{d}}}^{1/5}$ can only be continued along e_p from 0 to 0.1 and is linearly stable. Family ${\mathrm{I}_{\mathrm{r}}}^{1/5}$ can be continued along e_p from 0 to 0.75, and the orbits are linearly stable except $e_p \in [0.2, 0.65]$. The reason for the bifurcations from stability to instability when e_p grows, as well as the existence and stability of such periodic orbits with the variation of μ, deserves consideration in the future.

3.1.2 Case $\mu \neq 0.5$

There is only one useful time-reversing symmetry $\mathscr{R}_1$ for the nonplanar symmetric periodic orbits in the Hamiltonian (2) if $\mu \neq 0.5$. Consider the numerical study of such periodic orbits in the Sun–Jupiter ERTBP. Set $\mu = 0.99905$ and $e_p = 0.05$. As is stated in Proposition 1, there exist nearly circular periodic orbits of high inclination for any μ with k large enough. It is interesting to know whether

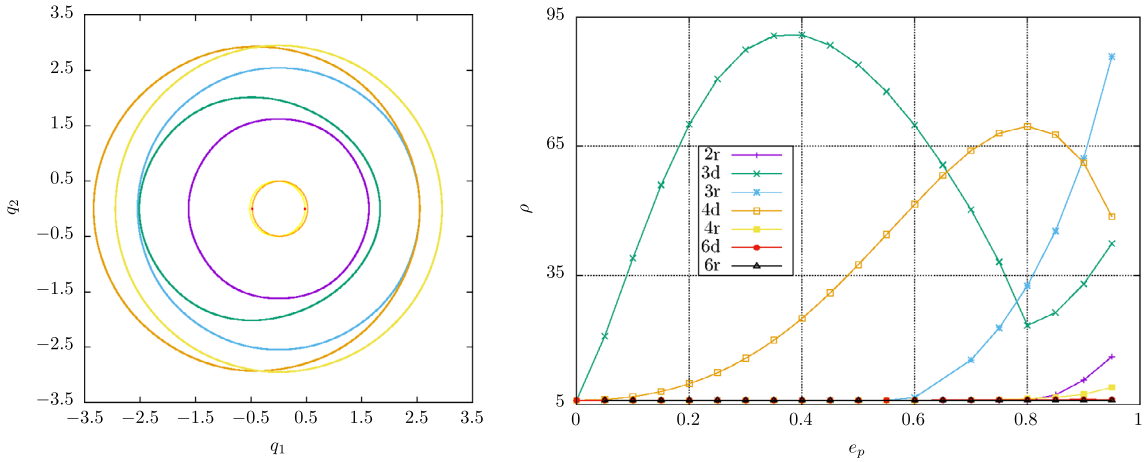

Fig. 4 The graphics of some $\mathscr{R}_1\mathscr{R}_2$-symmetric periodic orbits with $\mu = 0.5$ and $j = 1, 2 \le k \le 6$. "kd" and "kr" represent the type of periodic orbits with $n = 1/k$ and $n = -1/k$, respectively. The approximate initial value of q_1 is $k^{2/3}$. The left subgraph contains 5 periodic orbits, which are of type "2r", "3d", "4r", "5d", and "5r". The right subgraph contains 7 curves for the $e_p - \rho$ relations, and the types of the families can be referred to the legend

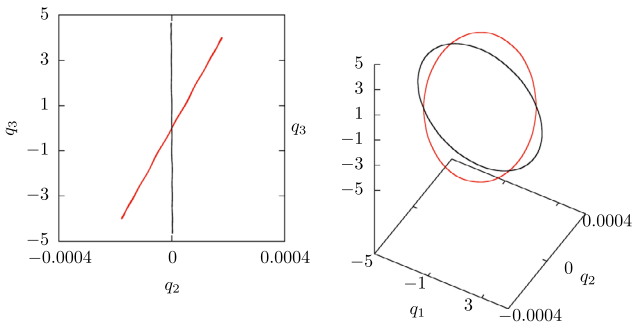

Fig. 5 Two examples of the comet-type symmetric periodic orbits with $\mu = 0.99905$, $e_p = 0.05$ in Table 2. The larger orbit is of the case "$(1/10, +, +, +)$", and the smaller orbit is of the case "$(1/8, -, -, +)$". The data are of 10 periods

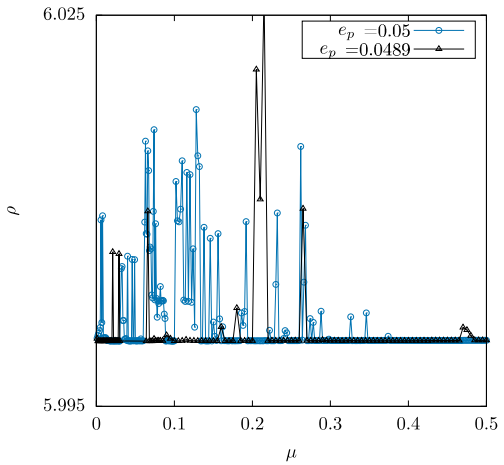

Fig. 6 The diagram of the relation between the stability index ρ of the nearly circular periodic orbits of type $(1/8, +, -, +)$ and the mass ratio μ. One curve is for $e_p = 0.05$, and the other is for $e_p = 0.0489$

such orbits still exist for k small and whether they are stable. To this end, we conduct numerical research and find that such orbits can be calculated with the accuracy 10^{-5} when $k \ge 7$. The numerical results show that it is possible to accurately calculate such periodic orbits when k is large. Such periodic orbits become closer to the u_1u_3-plane as k increases. In Table 2, there are 8 sets of period ratios and $j/k = 1/7, 1/8, 1/9, 1/10, 1/20, 1/98, 1/100, 1/102$. For each ratio j/k, 4 sets of initial values of the periodic orbits are supplied. Two periodic orbits are shown in Fig. 5 as examples. One orbit is of the type "$(1/8, -, -, +)$", and the other orbit is of the type "$(1/10, +, +, +)$".

The mass ratio μ can be used as one parameter to continue the periodic orbits. Let $e_p = 0.05, 0.0489$ be fixed successively. The periodic orbits of the type "$(1/8, +, -, +)$" are numerically continued from $\mu = 0.001$. The program fails at some values of μ, and these values are omitted. The relation between μ and ρ is shown in Fig. 6. It is obvious that the linear stability of these periodic orbits are affected by mass ratio μ, eccentricity e_p, the period ratio j/k, and the direction of the motion.

3.2 Hill-type

Consider the numerical continuation of the Hill-type nearly circular orbits close to the u_1u_3-plane. As far as we know, there is rarely any numerical work on the Hill-type high-inclination nearly circular periodic orbits in the ERTBP. It is interesting to consider the ERTBP with the background of the Sun–Jupiter and Uranus–Sun systems. Set $1 - \mu_1 =$ 9.5E-3 and $\mu_2 =$ 4.36E-5, respectively. e_p is taken as the approximate value 0.05. The initial values can be set as $|q_1| = a = \mu^{1/3}(k/j)^{2/3}$, $|p_3| = (\mu/a)^{1/2}$ and $|\cos E_p| = 1$. As the existence proof demands the perturbation to be sufficiently small, the value j/k should be big correspondingly.

Table 2 Continuation results for the comet-type symmetric periodic orbits with $1-\mu = 0.00095$, $e_p = 0.05$ and $j = 1$, $7 \le k \le 10$ and $k = 98, 100, 102$. The initial values are of the type in (10). ρ is the linear stability index, and the accuracy is the infinity norm of the deviation of the periodic orbit after one period

$j/k, q_1, p_3, \cos E_p$	q_1	p_2	p_3	$\rho - 6$, accuracy
1/7, +, −, +	3.6592987489638045	-6.4122106664957639E-6	-0.52276292935825519	4.5E-5, 3.4E-6
1/7, +, −, −	3.6591852291889055	1.0076050086637359E-4	-0.52278090168470115	7.6E-11, 3.4E-5
1/7, −, −, +	-3.6595666847189361	-3.2300482393227901E-5	-0.52272807327828696	7.7E-8, 6.0E-7
1/7, −, −, −	-3.6593683804109562	7.1231378413774948E-5	-0.52275293163232239	2.0E-5, 6.6E-8
1/8, +, −, +	3.9999626164658486	5.4210230072135188E-6	-0.50000815457236969	-7.0E-13, 2.4E-5
1/8, +, −, −	4.0000277329652985	-1.0675289545006397E-5	-0.50000085931580929	4.5E-10, 8.7E-6
1/8, −, −, +	-4.0000202855245481	-2.0981961398261546E-5	-0.50000289781015694	4.7E-6, 3.4E-7
1/8, −, −, −	-4.0001167463886214	1.3164858321973209E-5	-0.49998897137431436	3.8E-6, 1.3E-7
1/9, +, −, +	4.3267629076041452	-4.2072242537383840E-6	-0.48075125353714027	1.3E-10, 1.3E-5
1/9, +, −, −	4.3266440426180015	3.8504442837501964E-7	-0.48076495402763586	7.8E-13, 1.8E-5
1/9, −, −, +	-4.3267305692889710	-1.2215042323670958E-6	-0.48075606420853845	9.2E-6, 1.3E-6
1/9, −, −, −	-4.3288988459465712	1.6612736631431054E-5	-0.48051413042648866	1.8E-5, 1.7E-7
1/10, +, +, +	4.6416235211720576	-1.8255832376417327E-6	0.46415797351004001	8.4E-11, 1.3E-5
1/10, +, +, −	4.6413456440981653	3.3455256764516010E-7	0.46418603155250421	1.3E-10, 1.2E-5
1/10, −, +, +	-4.6415781139089827	8.5046069498431707E-7	0.46416333821269673	3.0E-6, 1.5E-7
1/10, −, +, −	-4.6416121804638824	3.6213273309066630E-6	0.46415926249244560	3.0E-6, 1.5E-7
1/20, +, −, +	7.3680746717162817	-1.5143641768103586E-7	-0.36840340580681524	3.8E-11, 4.9E-6
1/20, +, −, −	7.3680741127370055	-2.6168791635074620E-7	-0.36840344122687169	3.9E-11, 5.0E-6
1/20, −, +, +	-7.3680684952906841	1.4396331223650695E-7	0.36840380525882260	7.9E-7, 3.0E-8
1/20, −, +, −	-7.3682811593858473	7.1276108315551053E-7	0.36839313893333769	8.0E-7, 3.0E-8
1/98, +, +, +	21.256126128123359	6.3714527689866642E-11	0.21689923786405826	-3.0E-12, 1.2E-7
1/98, +, +, −	21.256120725000279	-1.8453113367049422E-9	0.21689929324465840	-5.6E-13, 6.0E-7
1/98, −, +, +	-21.256123958837428	2.7296604705071015E-9	0.21689926198175488	3.4E-8, 7.7E-10
1/98, −, +, −	-21.254842683643524	4.9618229495974987E-9	0.21691233656799166	2.4E-7, 8.0E-10
1/100, +, +, +	21.544346217477752	2.6390049362847486E-8	0.21544353364798838	1.7E-12, 6.1E-7
1/100, −, +, +	21.544360207168584	-2.3628401219165148E-9	0.21544339372326538	3.0E-12, 5.9E-7
1/100, +, +, −	-21.544351198669208	1.9133191503697579E-9	0.21544348546301900	3.2E-8, 7.3E-10
1/100, −, +, −	-21.544349146414532	2.2950806672727712E-9	0.21544350593492809	3.2E-8, 7.3E-10
1/102, +, +, +	21.830657231715431	-2.8296610120786632E-9	0.21402607808699303	3.3E-12, 5.7E-7
1/102, +, −, +	21.830658742953297	-7.1405922187972318E-9	-0.21402606325850704	1.1E-12, 5.8E-7
1/102, +, +, −	-21.830653628529703	2.3656707874384857E-9	0.21402611520715312	-7.3E-13, 2.2E-7
1/102, −, +, −	-21.830653085533680	1.5878119283864102E-11	0.21402612025433271	3.1E-8, 7.0E-10

However, if j is big, the integration spends more time as the step size is small. For the case $\mu = \mu_1$, the mild values $j/k = 15/1, 20/1$ are chosen as examples. The smaller values are tested, and $j = 9$ is the smallest value that can be used for the continuation.

In Xu and Fu (2009) the existence of the Hill-type nearly circular periodic orbits in the Uranus–Sun ERTBP is discussed. It is difficult to use the periodic ratio between the orbit of a main satellite and the orbit of Uranus as the small parameter k/j, as j/k may be bigger than 2000 in the real case. For the case $\mu = \mu_2$, periodic orbits are found within the accuracy 10^{-6} when $j/k = 100$. A numerical experiment confirms that there exist such periodic orbits, and their stability depends on the initial values and the related parameters. The numerical results are listed in Table 3. The graphics of such periodic orbits are like the one shown in Fig. 7 with $j/k = 15/1$.

Consider the elliptic Hill lunar problem. The Hamiltonian is

$$\mathcal{H}^{\mathtt{EHill}} = \frac{1}{2}\|\mathbf{y}\|^2 - \frac{1}{\|\mathbf{x}\|} - \frac{\|\mathbf{x}\|^2}{\|\boldsymbol{d}(t)\|^3}\mathscr{P}_2(\cos\theta). \tag{16}$$

The approximate initial values can be set as $\left((k/j)^{\frac{2}{3}}, 0, 0, 0, 0, (j/k)^{\frac{1}{3}}\right)$ if $\varepsilon^3 = k/j$. In Table 4, a few sets of initial val-

Table 3 Continuation results for the Hill-type symmetric periodic orbits with $e_p = 0.05$, $\mu_1 = 0.99905$,$\mu_2 = 4.36\text{E-}5$

$\mu, \frac{j}{k}, q_1, p_3, \cos E_p$	q_1	p_2	p_3	Accuracy
$\mu_1, 9/1, -, -, +$	0.23104753163817912	8.0620636981595163E-6	2.0794376956090326	7.6E-6
$\mu_1, 10/1, +, +, -$	0.21537709084179013	-4.7390796697328394E-5	2.15374689229495662	3.0E-7
$\mu_1, 15/1, +, +, +$	0.16436341432551488	5.0036877441153105E-6	2.4654262085761807	1.3E-7
$\mu_1, 15/1, +, -, +$	0.16436367968929597	3.9499901833411442E-6	-2.4654222443177933	2.3E-6
$\mu_1, 15/1, -, -, +$	-0.16436286895570323	-1.8913624401571552E-7	-2.4654287841629947	1.3E-7
$\mu_1, 15/1, +, -, -$	0.16436338845142534	3.9503115156928243E-6	-2.4654265954695549	1.4E-7
$\mu_1, 15/1, -, +, -$	-0.16436246794895698	8.4392190553698161E-6	2.4654347991509216	1.3E-7
$\mu_1, 20/1, +, +, +$	0.13567857291598950	1.8266566226512722E-6	2.7135520510913653	3.2E-8
$\mu_1, 20/1, +, -, +$	0.13567810115684364	-2.8338983017714020E-6	-2.7135614861419906	3.2E-8
$\mu_1, 20/1, -, -, +$	-0.13567823018764408	1.5202401461046449E-7	-2.7135566894273957	3.2E-8
$\mu_1, 20/1, +, +, -$	0.13567682577006848	-1.4976898593297709E-6	2.7135836228834762	3.2E-8
$\mu_1, 20/1, -, +, -$	-0.13567845037069237	1.1084871724569170E-5	2.7135526140754811	3.2E-8
$\mu_2, 100/1, +, +, +$	1.6336500706172479E-3	1.2935495288346786E-13	0.16338441652396937	-2.3E-7
$\mu_2, 100/1, +, -, +$	1.6324114759488188E-3	7.2954138446461076E-4	-0.16350664803264217	-4.0E-7
$\mu_2, 100/1, -, +, +$	-1.6335856889559293E-3	-1.3774201523538131E-4	0.16339072873300489	2.6E-7
$\mu_2, 100/1, -, -, +$	-1.6332904221876856E-3	-1.4261424806548357E-4	-0.16342024401880687	2.6E-7
$\mu_2, 100/1, +, -, -$	1.6337533424654455E-3	-7.8121392249276981E-7	-0.16337033074651763	-2.1E-7
$\mu_2, 100/1, -, +, -$	-1.6337180193249647E-3	-2.5687716281726035E-4	0.16337370558143691	-1.6E-6

Table 4 Continuation results for the Hill-type symmetric periodic orbits with $e_p = 0.05$

$j/k, q_1, p_3, E_p$	q_1	p_2	p_3	Accuracy
$9/1, +, \pm, +$	0.23027985156386710	-0.11923921522343746	$\pm$2.1030048386591433	6.5E-11
$9/1, -, +, +$	-0.23027985159772291	0.11923922447889911	2.1030048378295447	2.9E-10
$10/1, +, \pm, +$	0.21441595110081965	-0.12263152645883330	$\pm$2.1817641137275761	2.0E-10
$10/1, -, -, +$	-0.22971398774971366	0.13034344853460289	-2.1131087306366378	2.1E-9
$100/1, +, +, +$	4.6413955052640225E-2	-2.7355878060220995E-2	4.6421463857660310	5.0E-8
$100/1, +, -, +$	4.6413955429244334E-2	-2.7355870865517117E-2	-4.6421463481544718	4.0E-8
$100/1, -, +, +$	-4.6413955751133197E-2	2.7345266290028071E-2	4.6421463784576762	2.7E-8
$100/1, -, -, +$	-4.6413955682293610E-2	2.7344271595776716E-2	-4.6421463911971408	2.3E-8

ues of the spacial nearly circular periodic orbits of the elliptic Hill lunar problem are shown, where the period ratios are $k/j = 1/9, 1/10, 1/100$, and $e_p = 0.05$ is fixed. It is interesting to consider the central primary to be oblate, and the equator plane coincides with the reference plane. Denote the radius of the equator of the central planet as $a_e < \|\mathbf{x}\|$. The perturbation term about the oblateness is $-J_2 \frac{a_e^2}{\|\mathbf{x}\|^3} \mathscr{P}_2(\frac{x_3}{\|\mathbf{x}\|})$, where J_2 is the coefficient of the oblateness. The related research will be done in the future.

4 Conclusion

This paper mainly considers the numerical computation of the nearly circular periodic orbits with inclinations near 90° in the ERTBP. Both comet and Hill-type periodic orbits are calculated. Some propositions about the existence and linear stability of such symmetric orbits are introduced to be self-consistent. The linear stability of these periodic orbits is estimated by the index ρ, which is the sum of the moduli of the characteristic multipliers. When $\mu = 0.5$, twenty values of j/k are used to investigate the families of the comet-type doubly symmetric periodic orbits. The sets of initial values of these periodic orbits and the values of ρ are listed in Table 1 with $e_p = 0.05$. The graphics of two orbits are in Fig. 1 and Fig. 2. The diagram of ρ and e_p for some families can be referred to in Fig. 3. Some planar symmetric periodic orbits of $\mu = 0.5$ are also numerically studied in Fig. 4. When $\mu = 0.99905$ and $e_p = 0.05$, 32 sets of initial values of the comet-type symmetric periodic orbits are supplied in Table 2. When k/j increases, such periodic orbits become closer to the u_1u_3-plane, see Fig. 5. If k is small, periodic orbits cannot be continued with a good precision.

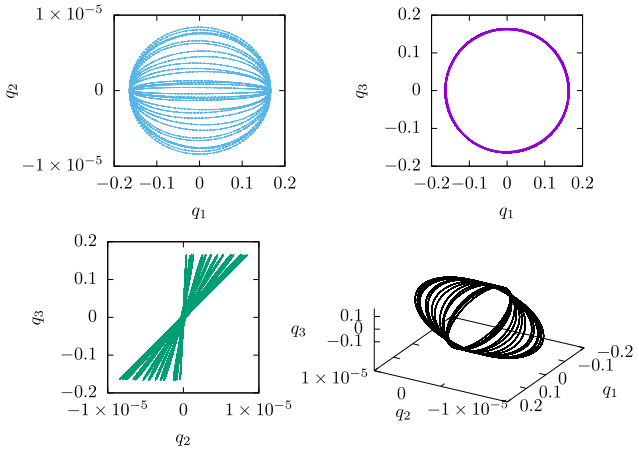

Fig. 7 The Hill-type symmetric periodic orbit with $\mu = 0.00095$ is nearly circular and of high inclination. The initial values are from case "$(15/1, + + +)$" in Table 3. The data is within one period 2π

The mass ratio can also be served as one parameter, as one example in Fig. 6, the family "$(1/8, +, -, +)$" is continued along $\mu \in [0, 0.5]$ with e_p fixed as 0.05 and 0.0489 separately. It is obvious that e_p and μ are crucial for the stability of the periodic orbits. Hill-type orbits are different from the comet-type ones. The j in the period ratio j/k cannot be too small to continue successfully, see Table 3. When calculating the Hill-type orbits with the mass of the central primary μ small, it is better to use the Hill lunar model. Some periodic orbits are calculated, and the initial values are given in Table 4.

Unlike the analysis and proofs, the numerical exploration concerns the accuracy of the initial values with great detail. It is interesting to use the Lindstedt-Poincaré method to give the approximate solutions of such periodic orbits and compare the approximate analytical solutions with the numerical results. It also makes sense to use the e_p and μ as small parameters to analytically study the linear stability of these orbits. It is still a puzzle to study the orbits of the planets. It is possible to continue the periodic orbits of the ERTBP to the full three-body problem and explain the existence of high-inclination orbits in the exoplanetary systems. The stability of these periodic orbits with a real astronomy background is very interesting for future research.

Acknowledgements This first author is supported by the National Nature Science Foundation of China (NSFC, Grant No. 11703006). The second author is supported by Shanghai Observatory's key cultivation project (N20210601003), Civil Aerospace "14th Five-Year" Technology Pre-research Project (KJSP2020020203). The authors would like to thank the reviewers of this paper for their constructive comments and suggestions.

Author contributions The first author Xu wrote the paper and calculated the results and contributed most of the ideas. The second author supplied some background for this paper and gave some suggestions. All authors reviewed the manuscript.

Declarations

Competing interests The authors declare no competing interests.

References

Bolotin, S.: Celest. Mech. Dyn. Astron. **93**, 343 (2015)
Broucke, R.A.: Celest. Mech. Dyn. Astron. **81**, 321 (2001)
Broyden, C.G.: Math. Comput. **19**, 577(92) (1965)
Chenciner, A.: Henri Poincaré, 1912–2012 In: Duplantier, B., Rivasseau, V. (eds.) Poincaré and the Three-Body Problem. Birkhäuser, Basel (2015)
Cors, J.M., Pinyol, C., Soler, J., Physica, D.: Nonlinear Phenom. **154**, 3–4 (2001)
Cors, J.M., Pinyol, C., Soler, J.: J. Differ. Equ. **219**, 1 (2005)
Farantos, S.C.: Comput. Phys. Commun. **108**(2–3), 240 (1998)
Galan-Vioque, J., Almaraz, F.J.M., Macías, E.F.: Eur. Phys. J. Spec. Top. **223**, 2705 (2014)
Gómez, G., Ollé, M.: Celest. Mech. **39**, 33 (1986)
Gomez, G., Olle, M.: Celest. Mech. Dyn. Astron. **52**, 107 (1991)
Haghighipour, N., Dvorak, R., Pilat-Lohinger, E.: In: Haghighipour, N. (ed.) Planetary Dynamics and Habitable Planet Formation in Binary Star Systems, p. 285. Springer, Dordrecht (2010)
Hénon, M.: Generating Families in the Restricted Three-Body Problem. Springer, Berlin (1997)
Koh, D., Anderson, R.L., Bermejo-Moreno, I.: J. Astronaut. Sci. **68**, 172 (2021)
Kotoulas, T., Voyatzis, G.: Astron. Astrophys. **441**, 807 (2005)
Llibre, J., Piñol, C.: Celest. Mech. Dyn. Astron. **48**, 319 (1990)
Meyer, K.R., Hall, G.R., Offin, D.: Introduction to Hamiltonian Dynamical Systems and the N-Body Problem. Springer, Berlin (2009)
Ollé, M., Pacha, J.R.: Astron. Astrophys. **351**, 1149 (1999)
Palacián, J.F., Yanguas, P., Fernández, S., Nicotra, M.A.: Phys. D: Nonlinear Phenom. **213**(1), 15 (2006)
Pan, S.S., Hou, X.Y.: Res. Astron. Astrophys. **22**, 072002 (2022)
Peng, H., Xu, S.J.: Celest. Mech. Dyn. Astron. **123**(3), 279 (2015)
Peng, H., Bai, X.L., Xu, S.J.: Commun. Nonlinear Sci. Numer. Simul. **47**, 1 (2017)
Press, W.H., Teukolsky, S.A., Vetterling, W.T., Flannery, B.P.: Numerical Recipes in Fortran 77, the Art of Scientific Computing. Cambridge University Press, New York (1992)
Sarris, E.: Astrophys. Space Sci. **162**, 107 (1989)
Sheth, D., Thomas, V.O.: Astrophys. Space Sci. **367**, 99 (2022)
Szebehely, V.G.: Theory of Orbits. Academic Press, New York (1967)
Tsirogiannis, G.A., Perdios, E.A., Markellos, V.V.: Celest. Mech. Dyn. Astron. **103**(1), 49 (2009)
Voyatzis, G., Gkolias, I., Varvoglis, H.: Celest. Mech. Dyn. Astron. **113**(1), 125 (2012)
Xu, X.-B.: Chin. Astron. Astrophys. **64**(4), 40 (2022)
Xu, X.-B.: Celest. Mech. Dyn. Astron. **135**, 8 (2023). https://doi.org/10.1007/s10569-023-10121-y
Xu, X.-B., Fu, Y.-N.: Sci. China Ser. G **52**(9), 1404 (2009)
Zhao, L.: Math. Ann. (2021). https://doi.org/10.1007/s00208-021-02339-8